Striping of nematic elastomers

Eliot Fried & Vladimir Korchagin

Department of Theoretical and Applied Mechanics, University of Illinois,
Urbana, IL 61801-2935, USA

We consider a recent experiment of Kundler & Finkelmann (1995), who subjected an aligned specimen of nematic elastomer to uniaxial extension and observed the formation of striped domains. Working with an energy density that combines the effects included in the neo-Hookean theory of nematic rubber elasticity with the Oseen–Zöcher–Frank theory of nematic curvature-elasticity and assuming that the deformation and orientation fields remain in-plane, we arrive at a boundary-value problem which admits solutions corresponding to striped states. We use bifurcation theory to explore the local stability of these solutions. We also obtain analytical estimates for the energy and thickness of interstripe domain walls as functions of imposed extension and compare these with numerical predictions.

---

1. Introduction

A *nematic elastomer* is a rubber-like solid formed by the cross-linking of a polymeric fluid which includes liquid crystalline molecules as elements of its main chain and/or as pendant side groups. Like nematic liquid crystals, these materials possess local orientational order but lack the long-range translational order of crystalline solids.

Here, we focus on the analysis of an experiment performed by Kundler & Finkelmann (1995). The specimens used in this experiment were prepared by a two-step cross-linking reaction. Liquid-crystalline mesogens and the two cross-linking components were added to poly[oxy(methylsilylene)] in a solution of toluene. In the first reaction step, a weakly cross-linked network was formed. After removing the solvent, a uniaxial nematic phase was formed. The network was then subjected to an external mechanical stress and additional cross-links were formed, resulting in a uniaxial nematic elastomer with known step-length anisotropy. The specimens used in the experiment were very thin rectangular sheets with in-plane lengths of 100 mm along the axis of the load and 70 mm perpendicular to the axis of the load. To study the interaction between loading and nematic orientation, these specimens were cut at various angles to the nematic axis. We focus on the case where the specimens were cut with the nematic axis in-plane and perpendicular to the axis of the load. In this situation, Kundler & Finkelmann (1995) found that the transparent monodomain present in the uniaxially-aligned nematic state breaks up into an opaque polydomain structure with striped domains realigning clockwise and counterclockwise towards the axis of the load. While gross simple shear is suppressed by the clamps on the specimen, it appears that simple shear is present in each striped domain. Kundler & Finkelmann (1995) observed the existence of strain threshold of ~ 1.1 below which reorientation does not occur and measured a characteristic stripe width of ~ 15 μm. Subsequent to the work of Kundler & Finkelmann (1995), Roberts, Mitchell & Davis (1997) observed that when stretch is applied perpendicular to the nematic axis of an acrylate-based nematic elastomer, the orientation switches discontinuously, without

evidence of localized inhomogeneities or domain formation. In the wake of this controversy, Talroze et al. (1998) and Zubarev et al. (1999) conducted an exhaustive series of experiments with an acrylate-based elastomer and found that, depending on the geometrical aspect ratio of the specimen, both scenarios are possible. Specifically, when the sample is long in the direction of loading, the scenario of a homogeneous orientation switch is realized, whereas when the sample is short, the scenario of a striped pattern formation is realized.

In the present work, we rely on a particular expression for the energy density. This expression combines the effects of the neo-Hookean theory of nematic rubber elasticity with the Oseen–Zöcher–Frank theory of nematic curvature elasticity. We assume that the deformation is a plane strain involving a uniform stretch along the axis of loading, a uniform contraction along the axis of referential orientation, and a shear within the plane defined by these two axes. Further, we assume that, during the process of stretching and reorientation, the nematic orientation remains within the plane defined by the axes of loading and referential orientation. Our formulation leads to a boundary-value problem for the shear and director angle. We find that inhomogeneous solutions to this boundary-value problem correspond to striped states. Using bifurcation theory, we study the local stability of inhomogeneous solutions. We also obtain analytical estimates for the thickness and energy of an interstripe layer. These estimates show that the thickness of a layer is independent of the number of stripes present in the specimen but that the energy of a layer varies depending on the number of stripes present. This variation occurs due because the amplitude of the angle that describes the orientation field depends upon the number of stripes present. We also use numerical methods to solve the boundary-value problem. For physcially relevant choices of the material parameters, we compute solutions to the boundary-value problem and use these solutions to determine the thickness and energy of a single interstripe layer. Despite the approximate nature our the analytical estimates, we find that these compare favorably with the numerical results.

Previously, the problem of striping in a nematic elastomer has been considered previously by Verwey, Warner & Terentjev (1996). This work differs from ours in two main features. First, and most importantly, Verwey, Warner & Terentjev (1996) work with an energy density that includes a gradient term which is not properly invariant under superposed rigid changes of observer. Here, we require thaat the energy density is properly invariant. As an interesting consequence of this requirement, we find that the thickness of an interstripe layer depends upon the axial extension of the specimen. A second difference is that Verwey, Warner & Terentjev (1996) rely on a variational description of equilibrium. Here, we work directly with the equations of equilibrium. Hence, while the solution of our problem involves the determination of a pressure field necessary to ensure the constraint of incompressibility, this consideration is completely absent from the analysis of Verwey, Warner & Terentjev (1996).

2. Preliminaries

We consider an incompressible nematic-elastomeric body that, in a reference state, occupies a region $\mathcal{R}$ in a three-dimensional Euclidean point space $\mathcal{E}$. To describe the macroscopic kinematics, we introduce a deformation $\boldsymbol{y}$ which assigns to each point $\boldsymbol{x}$ of $\mathcal{R}$ a point $\boldsymbol{y}(\boldsymbol{x})$ of $\mathcal{E}$. We write $\boldsymbol{F} = \operatorname{Grad} \boldsymbol{y}$ for the deformation gradient and, due to the incompressibility of the medium, require that $\det \boldsymbol{F} = 1$. To describe the microstructural kinematics, we introduce a step-length $\boldsymbol{L}$ which assigns to each point $\boldsymbol{x}$ in $\mathcal{R}$ a symmetric and positive-definite tensor $\boldsymbol{L}(\boldsymbol{x})$ that describes any nematically-induced distortion of the polymer chains.

3. Constitutive assumptions

The molecular-statistical theory of Warner, Gelling & Vilgis (1988) yields an expression,

$$\psi_{\rm bulk} = \frac{\mu}{2}\big(\mathrm{tr}(\boldsymbol{L}^{-1/2}\boldsymbol{F}\boldsymbol{L}_0\boldsymbol{F}^{\top}\boldsymbol{L}^{-1/2}) + \log\det(\boldsymbol{L}^{-1}\boldsymbol{L}_0) - 3\big), \tag{3.1}$$

for the bulk energy-density of an incompressible nematic elastomer in terms of $\boldsymbol{F}$ and $\boldsymbol{L}$. Appearing in (3.1) are two material parameters—the step-length $\boldsymbol{L}_0$ in the reference state and the shear modulus $\mu > 0$. Like $\boldsymbol{L}$, $\boldsymbol{L}_0$ takes only symmetric and positive-definite values.

In the specimens used by Kundler & Finkelmann (1995), $\boldsymbol{L}_0$ has the uniaxial form

$$\boldsymbol{L}_0 = \ell_\perp\boldsymbol{1} + (\ell_\parallel - \ell_\perp)\boldsymbol{n}_0\otimes\boldsymbol{n}_0, \tag{3.2}$$

where $\boldsymbol{n}_0$, with $|\boldsymbol{n}_0| = 1$, determines the nematic orientation in the undeformed reference state and $\ell_\perp > 0$ and $\ell_\parallel > 0$ are the molecular step-lengths perpendicular and parallel to the orientation. Motivated by the experimental observations, we restrict attention to situations where, in the deformed state, the medium remains uniaxial and the molecular step-lengths are unaltered; then, $\boldsymbol{L}$ has the form

$$\boldsymbol{L} = \ell_\perp\boldsymbol{1} + (\ell_\parallel - \ell_\perp)\boldsymbol{n}\otimes\boldsymbol{n}, \tag{3.3}$$

where $\boldsymbol{n}$, with $|\boldsymbol{n}| = 1$, determines the nematic orientation in the deformed state.

In view of (3.2) and (3.3), we introduce the step-length anisotropy

$$s = \frac{\ell_\parallel}{\ell_\perp} > 0 \tag{3.4}$$

and expand (3.1) to give

$$\psi_{\rm bulk} = \frac{\mu}{2}\Big(|\boldsymbol{F}|^2 - \frac{s-1}{s}|\boldsymbol{F}^{\top}\boldsymbol{n}|^2 + (s-1)|\boldsymbol{F}\boldsymbol{n}_0|^2 - \frac{(s-1)^2}{s}(\boldsymbol{F}^{\top}\boldsymbol{n}\cdot\boldsymbol{n}_0)^2 - 3\Big). \tag{3.5}$$

The energy density (3.5) describes the material response in regions in which $\boldsymbol{n}$ is homogeneous—as may be the case within individual stripes. To account for variations of $\boldsymbol{n}$ that occur across transition layers separating stripes, we introduce a gradient-energy density

$$\psi_{\rm grad} = \frac{\kappa(s-1)^2}{2s}|\boldsymbol{F}^{\top}\boldsymbol{G}|^2, \tag{3.6}$$

with $\boldsymbol{G} = \mathrm{Grad}\,\boldsymbol{n}$. This expression arises on setting $k_1 = k_2 = k_3 = \kappa(s-1)^2/2s$ and $k_4 = 0$ in the generalization†

$$\begin{aligned}&\tfrac{1}{2}(k_1 - k_2 - k_4)(\boldsymbol{F}\cdot\boldsymbol{G})^2 + \tfrac{1}{2}(k_3 - k_2 - k_4)|\mathrm{sym}(\boldsymbol{F}^{\top}\boldsymbol{G})\boldsymbol{n}_0|^2\\ &\qquad + \tfrac{1}{2}(k_2 + k_4)|\boldsymbol{F}^{\top}\boldsymbol{G}|^2 - \tfrac{1}{4}k_4\big(\big(\mathrm{ax}(\boldsymbol{n}_0)\cdot(\boldsymbol{F}^{\top}\boldsymbol{G})\big)^2 + \big(\mathrm{ax}(\boldsymbol{F}^{\top}\boldsymbol{n})\cdot(\boldsymbol{F}^{\top}\boldsymbol{G})\big)^2\big)\end{aligned} \tag{3.7}$$

of the Oseen–Zöcher–Frank energy density for uniaxial nematic elastomers with orientations $\boldsymbol{n}_0$ and $\boldsymbol{n}$ in the reference and deformed states (Anderson et al., 1999). We refer to $\kappa > 0$ as the Frank modulus.

† Here, $\mathrm{sym}\boldsymbol{A}$ denotes the symmetric component of the tensor $\boldsymbol{A}$ and $\mathrm{ax}(\boldsymbol{v})$ denote the axial tensor of v, i.e., the unique skew tensor with the property that $\big(\mathrm{ax}(\boldsymbol{v})\big)\boldsymbol{u} = \boldsymbol{v}\times\boldsymbol{u}$ for all $\boldsymbol{u}$.

Summing (3.5) and (3.6) yields an expression,

$$\begin{aligned}\psi &= \hat{\psi}(\boldsymbol{F},\boldsymbol{n},\boldsymbol{G})\\ &= \frac{\mu}{2}\Big(|\boldsymbol{F}|^2 - \frac{s-1}{s}|\boldsymbol{F}^{\top}\boldsymbol{n}|^2 + (s-1)|\boldsymbol{F}\boldsymbol{n}_0|^2 - \frac{(s-1)^2}{s}(\boldsymbol{F}^{\top}\boldsymbol{n}\cdot\boldsymbol{n}_0)^2 - 3\Big)\\ &\quad + \frac{\kappa(s-1)^2}{2s}|\boldsymbol{F}^{\top}\boldsymbol{G}|^2,\end{aligned} \tag{3.8}$$

for the total energy-density $\psi = \psi_{\rm bulk} + \psi_{\rm grad}$ as a function $\hat{\psi}$ of $\boldsymbol{F}$, $\boldsymbol{n}$, and $\boldsymbol{G}$.

On choosing the step-length anisotropy s equal to unity, (3.8) reduces to the conventional neo-Hookean energy density $\mu\big(|\boldsymbol{F}|^2-3\big)/2$. In this case, the step length is isotropic and the polymer molecules are random spherical coils. When s differs from unity, the molecules are ellipsoidal coils—oblate or prolate depending on whether s is less than or greater than unity, respectively.

4. Field equations

Bearing in mind the particular form (3.8) of the energy density, the deformational stress $\boldsymbol{S}$ is given (Anderson, Carlson & Fried 1999) by

$$\begin{aligned}\boldsymbol{S} &= \hat{\boldsymbol{S}}(\boldsymbol{F},\boldsymbol{n},\boldsymbol{G}) - p\boldsymbol{F}^{-\top}\\ &= \mu\Big(\boldsymbol{F} - \frac{s-1}{s}\boldsymbol{n}\otimes\boldsymbol{F}^{\top}\boldsymbol{n} + (s-1)\boldsymbol{F}\boldsymbol{n}_0\otimes\boldsymbol{n}_0 - \frac{(s-1)^2}{s}(\boldsymbol{F}^{\top}\boldsymbol{n}\cdot\boldsymbol{n}_0)\boldsymbol{n}\otimes\boldsymbol{n}_0\Big)\\ &\quad + \frac{\kappa(s-1)^2}{s}\boldsymbol{G}\boldsymbol{G}^{\top}\boldsymbol{F} - p\boldsymbol{F}^{-\top},\end{aligned} \tag{4.1}$$

with p a constitutively indeterminate pressure that reacts to the constraint $\det\boldsymbol{F} = 1$, while the internal orientational-force $\boldsymbol{\pi}$ and the orientational stress $\boldsymbol{\Sigma}$ are given by†

$$\boldsymbol{\pi} = -\hat{\pi}(\boldsymbol{F},\boldsymbol{n}) = \frac{\mu(s-1)}{s}(\boldsymbol{1}-\boldsymbol{n}\otimes\boldsymbol{n})\big(\boldsymbol{F}\boldsymbol{F}^{\top} + (s-1)\boldsymbol{F}\boldsymbol{n}_0\otimes\boldsymbol{F}\boldsymbol{n}_0\big)\boldsymbol{n} \tag{4.2}$$

and

$$\boldsymbol{\Sigma} = \hat{\boldsymbol{\Sigma}}(\boldsymbol{F},\boldsymbol{n},\boldsymbol{G}) = \frac{\kappa(s-1)^2}{s}(\boldsymbol{1}-\boldsymbol{n}\otimes\boldsymbol{n})\boldsymbol{F}\boldsymbol{F}^{\top}\boldsymbol{G}, \tag{4.3}$$

respectively.

On neglecting external body forces and restricting attention to equilibrium, $\boldsymbol{S}$, $\boldsymbol{\Sigma}$, and $\boldsymbol{\pi}$ must comply with the field equations

$$\mathrm{Div}\boldsymbol{S} = \boldsymbol{0} \qquad \text{and} \qquad \mathrm{Div}\boldsymbol{\Sigma} + (\boldsymbol{G}\cdot\boldsymbol{\Sigma})\boldsymbol{n} + \boldsymbol{\pi} = \boldsymbol{0}, \tag{4.4}$$

expressing deformational and orientational-force balance. Moment balance, which requires that the tensor $\boldsymbol{S}\boldsymbol{F}^{\top} + \boldsymbol{n}\otimes\boldsymbol{\pi} + \boldsymbol{\Sigma}\boldsymbol{G}^{\top}$ be symmetric, is guaranteed provided that $\hat{\psi}(\boldsymbol{Q}\boldsymbol{F},\boldsymbol{Q}\boldsymbol{n},\boldsymbol{Q}\boldsymbol{G}) = \hat{\psi}(\boldsymbol{F},\boldsymbol{n},\boldsymbol{G})$ for all rotations $\boldsymbol{Q}$. A direct calculation shows that the particular choice (3.8) of $\hat{\psi}$ possesses this invariance.

† As a consequence of the constraint $|\boldsymbol{n}| = 1$, the internal orientational-force and the orientational stress generally include both active and reactive components. Anderson, Carlson & Fried (1999) consider both the active and reactive components of these fields and explain why determination of the multipliers that arise in response to the constraint $|\boldsymbol{n}| = 1$ are of negligible importance. Here, we therefore consider only the constitutively determinate (i.e., active) components of the internal orientational-force and the orientational stress and denote these by $\boldsymbol{\pi}$ and $\boldsymbol{\Sigma}$.

5. Nondimensionalization

Using δ to denote a characteristic length, we observe that μ, κ, and δ yield a single dimensionless parameter‡

$$\epsilon = \frac{\kappa}{\mu\delta^2} > 0. \tag{5.1}$$

Labeling the unscaled fields with asterisks, we introduce the dimensionless independent and dependent variables

$$\boldsymbol{x} = \frac{\boldsymbol{x}^*}{\delta}, \qquad \boldsymbol{y}(\boldsymbol{x}) = \frac{\boldsymbol{y}^*(\boldsymbol{x}^*)}{\delta}, \qquad \boldsymbol{n}(\boldsymbol{x}) = \boldsymbol{n}^*(\boldsymbol{x}^*), \qquad p(\boldsymbol{x}) = \frac{p^*(\boldsymbol{x}^*)}{\mu}, \tag{5.2}$$

and constitutive response functions

$$\left.\begin{aligned} \hat{\psi}(\boldsymbol{F},\boldsymbol{n},\boldsymbol{G}) &= \frac{\hat{\psi}^*(\boldsymbol{F}^*,\boldsymbol{n}^*,\boldsymbol{G}^*)}{\mu}, \qquad \hat{\boldsymbol{S}}(\boldsymbol{F},\boldsymbol{n},\boldsymbol{G}) = \frac{\hat{\boldsymbol{S}}^*(\boldsymbol{F}^*,\boldsymbol{n}^*,\boldsymbol{G}^*)}{\mu}, \\ \hat{\boldsymbol{\pi}}(\boldsymbol{F},\boldsymbol{n}) &= \frac{\hat{\boldsymbol{\pi}}^*(\boldsymbol{F}^*,\boldsymbol{n}^*)}{\mu}, \qquad \hat{\boldsymbol{\Sigma}}(\boldsymbol{F},\boldsymbol{n},\boldsymbol{G}) = \frac{\hat{\boldsymbol{\Sigma}}^*(\boldsymbol{F}^*,\boldsymbol{n}^*,\boldsymbol{G}^*)}{\mu\delta}. \end{aligned}\right\} \tag{5.3}$$

From (3.8), (4.1), (4.2), (4.3), (5.2), and (5.3) it follows that

$$\left.\begin{aligned} \psi &= \frac{1}{2}\Big(|\boldsymbol{F}|^2 - \frac{s-1}{s}|\boldsymbol{F}^\top\boldsymbol{n}|^2 + (s-1)|\boldsymbol{F}\boldsymbol{n}_0|^2 - \frac{(s-1)^2}{s}(\boldsymbol{F}^\top\boldsymbol{n}\cdot\boldsymbol{n}_0)^2 - 3\Big) \\ &\quad + \frac{\epsilon(s-1)^2}{2s}|\boldsymbol{F}^\top\boldsymbol{G}|^2, \\ \boldsymbol{S} &= \boldsymbol{F} - \frac{s-1}{s}\boldsymbol{n}\otimes\boldsymbol{F}^\top\boldsymbol{n} + (s-1)\boldsymbol{F}\boldsymbol{n}_0\otimes\boldsymbol{n}_0 - \frac{(s-1)^2}{s}(\boldsymbol{F}^\top\boldsymbol{n}\cdot\boldsymbol{n}_0)\boldsymbol{n}\otimes\boldsymbol{n}_0 \\ &\quad + \frac{\epsilon(s-1)^2}{s}\boldsymbol{G}\boldsymbol{G}^\top\boldsymbol{F} - p\boldsymbol{F}^{-\top}, \\ \boldsymbol{\pi} &= \frac{(s-1)}{s}(\boldsymbol{1} - \boldsymbol{n}\otimes\boldsymbol{n})\big(\boldsymbol{F}\boldsymbol{F}^\top + (s-1)\boldsymbol{F}\boldsymbol{n}_0\otimes\boldsymbol{F}\boldsymbol{n}_0\big)\boldsymbol{n}, \\ \boldsymbol{\Sigma} &= \frac{\epsilon(s-1)^2}{s}(\boldsymbol{1} - \boldsymbol{n}\otimes\boldsymbol{n})\boldsymbol{F}\boldsymbol{F}^\top\boldsymbol{G}. \end{aligned}\right\} \tag{5.4}$$

Henceforth, we write $\mathcal{R}$ for the region associated with the dimensionless position $\boldsymbol{x}$, use Grad and Div to denote the gradient and divergence on $\mathcal{R}$, and work only with dimensionless quantities. The field equations are then (4.4) with $\boldsymbol{S}$, $\boldsymbol{\pi}$, and $\boldsymbol{\Sigma}$ as given in (5.4).

6. Specimen geometry. Kinematic assumptions

Referring to the experiment of Kundler & Finkelmann (1995), we select a right-handed Cartesian basis $\{\boldsymbol{e}_1, \boldsymbol{e}_2, \boldsymbol{e}_3\}$, with $\boldsymbol{e}_1$ parallel to the axis of loading and $\boldsymbol{e}_2 = \boldsymbol{n}_0$, and suppose that the region $\mathcal{R}$ occupied by the body in the undeformed reference state has the form

$$\mathcal{R} = \{\boldsymbol{x} : 0 < \boldsymbol{x}\cdot\boldsymbol{e}_1 < l_1, 0 < \boldsymbol{x}\cdot\boldsymbol{e}_2 < l, 0 < \boldsymbol{x}\cdot\boldsymbol{e}_3 < l_3\} \tag{6.1}$$

‡ If we take $\delta \sim 10^{-5}$ m, which is of the order of the characteristic stripe-width observed in the experiment of Kundler & Finkelmann (1995), and, following Verwey, Warner & Terentjev (1996), assume that $\mu \sim 10^5$ N/m^2 and that $\kappa \sim 10^{-11}$ N, (5.1) yields $\epsilon = 10^{-6}$.

of a rectangular sheet. We write $x = \boldsymbol{x}\cdot\boldsymbol{e}_2$ for the coordinate that lies in-plane and is perpendicular to the axis of loading.

We assume that

$$\boldsymbol{F} = f\boldsymbol{e}_1\otimes\boldsymbol{e}_1 + \frac{1}{f}\,\boldsymbol{e}_2\otimes\boldsymbol{e}_2 + \boldsymbol{e}_3\otimes\boldsymbol{e}_3 + \gamma\,\boldsymbol{e}_1\otimes\boldsymbol{e}_2, \tag{6.2}$$

which corresponds to a plane strain with uniform stretch f along the axis of loading and in-plane shear γ possibly dependent on x, and that

$$\boldsymbol{n} = (\sin\varphi)\,\boldsymbol{e}_1 + (\cos\varphi)\,\boldsymbol{e}_2, \tag{6.3}$$

which corresponds to a unit vector field in the plane of the undeformed specimen, with φ possibly dependent on x and taking values between $-\frac{\pi}{2}$ and $\frac{\pi}{2}$.†

On using (6.2) and (6.3) in $(5.4)_1$ and bearing in mind that $\boldsymbol{n}_0 = \boldsymbol{e}_2$, it follows that

$$\psi = \frac{(f^2-1)^2}{2f^2} + \tilde{\psi}(\gamma,\varphi,\varphi'), \tag{6.4}$$

where a superposed prime denotes differentiation with respect to x and

$$\tilde{\psi}(\gamma,\varphi,\varphi') = \frac{\gamma^2}{2} - \frac{s-1}{2}\Big(\frac{f^2\sin^2\varphi}{s} - \Big(\gamma\cos\varphi - \frac{\sin\varphi}{f}\Big)^2\Big) + \frac{\epsilon(s-1)^2}{2s}\Big(f^2\cos^2\varphi + \Big(\gamma\cos\varphi - \frac{\sin\varphi}{f}\Big)^2\Big)|\varphi'|^2. \tag{6.5}$$

As for $\boldsymbol{S}$, $\boldsymbol{\pi}$, and $\boldsymbol{\Sigma}$, a calculation analogous to that leading to (6.4) and (6.5) yields‡

$$\boldsymbol{S} = S_{\alpha\beta}\boldsymbol{e}_\alpha\otimes\boldsymbol{e}_\beta + S_{33}\boldsymbol{e}_3\otimes\boldsymbol{e}_3, \quad \boldsymbol{\pi} = \pi_\alpha\boldsymbol{e}_\alpha, \quad \text{and} \quad \boldsymbol{\Sigma} = \Sigma_{\alpha 2}\boldsymbol{e}_\alpha\otimes\boldsymbol{e}_2, \tag{6.6}$$

with

$$\left.\begin{aligned} S_{11} &= \frac{f}{s} + \frac{f(s-1)\cos^2\varphi\big(1+\epsilon(s-1)|\varphi'|^2\big)}{s} - \frac{p}{f},\\ S_{12} &= \gamma + \frac{(s-1)\cos\varphi\big(f\gamma\cos\varphi - \sin\varphi\big)\big(s+\epsilon(s-1)|\varphi'|^2\big)}{sf},\\ S_{21} &= -\frac{(s-1)f\sin\varphi\cos\varphi\big(1+\epsilon(s-1)|\varphi'|^2\big)}{s} + p\gamma,\\ S_{22} &= \frac{1}{f} - \frac{(s-1)\sin\varphi\big(f\gamma\cos\varphi - \sin\varphi\big)\big(s+\epsilon(s-1)|\varphi'|^2\big)}{sf} - pf,\\ S_{33} &= 1-p, \end{aligned}\right\} \tag{6.7}$$

† Due to considerations of material symmetry (Anderson, Carlson & Fried 1999), we do not distinguish between $\boldsymbol{n}$ and $-\boldsymbol{n}$.

‡ We employ the summation convention, with the indices α and β running over $\{1,2\}$.

and

$$\left.\begin{aligned}
\pi_1 &= \frac{(s-1)\cos\varphi}{s}\Big(\frac{s\gamma\cos 2\varphi}{f}+\Big(f^2+s\gamma^2-\frac{s}{f^2}\Big)\sin\varphi\cos\varphi\Big),\\
\pi_2 &= -\frac{(s-1)\sin\varphi}{s}\Big(\frac{s\gamma\cos 2\varphi}{f}+\Big(f^2+s\gamma^2-\frac{s}{f^2}\Big)\sin\varphi\cos\varphi\Big),\\
\Sigma_{12} &= \frac{\epsilon(s-1)^2\cos\varphi}{s}\Big((f^2+\gamma^2)\cos^2\varphi-\frac{2\gamma}{f}\sin\varphi\cos\varphi+\frac{\sin^2\varphi}{f^2}\Big)\varphi',\\
\Sigma_{22} &= -\frac{\epsilon(s-1)^2\sin\varphi}{s}\Big((f^2+\gamma^2)\cos^2\varphi-\frac{2\gamma}{f}\sin\varphi\cos\varphi+\frac{\sin^2\varphi}{f^2}\Big)\varphi'.
\end{aligned}\right\} \tag{6.8}$$

Granted that γ and φ vary at most with x, (6.5), $(6.6)_{2,3}$, and (6.8) imply that ψ, $\boldsymbol{\Sigma}$, and $\boldsymbol{\pi}$ also depend only on x. Similarly, unless p is found to depend on coordinates other than x, $(6.6)_1$ and (6.7) imply that $\boldsymbol{S}$ depends at most on x.

7. Boundary conditions

We require that the surfaces of the specimen with unit normal $\boldsymbol{e}_2$ be free of deformational traction, viz.,†

$$\boldsymbol{S}(0)\boldsymbol{e}_2=\boldsymbol{S}(l)\boldsymbol{e}_2=\boldsymbol{0}, \tag{7.1}$$

but allow for nontrivial deformational tractions on the remaining surfaces of the specimen.

In addition, we require that the orientational traction on the surfaces of the specimen with unit normal $\boldsymbol{e}_2$ be free of orientational traction, viz.,

$$\boldsymbol{\Sigma}(0)\boldsymbol{e}_2=\boldsymbol{\Sigma}(l)\boldsymbol{e}_2=\boldsymbol{0}. \tag{7.2}$$

From (6.8), it follows that the orientational tractions on the faces of the remaining surfaces of the specimen vanish.

8. Boundary-value problem

The deformational force balance $(4.4)_1$ together with the boundary conditions (7.1) require that $S_{12}=S_{22}=0$. Using $(6.7)_2$ and $(6.7)_4$, we therefore obtain relations,

$$\gamma=\frac{(s-1)\sin\varphi\cos\varphi\big(s+\epsilon(s-1)|\varphi'|^2\big)}{f\big(s\sin^2\varphi+s^2\cos^2\varphi+\epsilon(s-1)^2\cos^2\varphi|\varphi'|^2\big)} \tag{8.1}$$

and

$$p=\frac{s^2+\epsilon(s-1)^2|\varphi'|^2}{f^2\big(s\sin^2\varphi+s^2\cos^2\varphi+\epsilon(s-1)^2\cos^2\varphi|\varphi'|^2\big)}, \tag{8.2}$$

determining γ and p in terms of φ and φ'. Using these in $(6.7)_{1,3,5}$ yields expressions for S_{11}, S_{21}, and S_{33} in terms of φ and φ'. From (8.2), it follows that $\boldsymbol{S}$ varies only with x.‡

The orientational-force balance $(4.4)_2$ reduces to a single scalar ordinary differential

† Here, for simplicity, we suppress possible dependence of $\boldsymbol{S}$ on coordinates other than x.

‡ In general, S_{11}, S_{21}, and S_{33} are nonvanishing. However, if we interpret the kinematical Ansatz (6.2) as an internal constraint and introduce a reactive stress that responds to this constraint, this stress cancels S_{11}, S_{21}, and S_{33}, rendering the equilibrium state stress-free.

equation, which can be expressed concisely as

$$\Big(\frac{\partial\tilde{\psi}(\gamma,\varphi,\varphi')}{\partial\varphi'}\Big)' = \frac{\partial\tilde{\psi}(\gamma,\varphi,\varphi')}{\partial\varphi}. \tag{8.3}$$

In view of (8.1), (8.3) is a second-order ordinary-differential-equation for φ. Boundary conditions for φ follow from (7.2), which requires that

$$\varphi'(0) = \varphi'(l) = 0. \tag{8.4}$$

9. Solutions of the boundary-value problem

9.1. *Homogeneous solutions*

Homogeneous solutions of the boundary-value problem (8.3)–(8.4) are determined by the equation

$$\frac{\partial\tilde{\psi}(\gamma,\varphi,0)}{\partial\varphi} = \left(\frac{f^2}{s} - \frac{s^2}{f^2(\sin^2\varphi + s\cos^2\varphi)^2}\right)\sin\varphi\cos\varphi = 0, \tag{9.1}$$

which yields

$$\varphi = 0, \qquad \varphi = \pm\frac{\pi}{2}, \qquad \varphi = \pm\arcsin\left(\frac{1}{f}\sqrt{\frac{s(f^2-1)}{s-1}}\right). \tag{9.2}$$

Shears,

$$\gamma = 0, \qquad \gamma = 0, \qquad \gamma = \pm\frac{1}{f}\sqrt{\frac{(f^2-1)(s-f^2)}{s}}, \tag{9.3}$$

corresponding to the homogeneous solutions (9.2) of (8.3)–(8.4) are determined on using (9.2) in (8.1).

The relations $(9.2)_{3_\pm}$ and $(9.3)_{3_\pm}$ are valid if $0 < s < 1$ and $\sqrt{s} < f < 1$, which coincides with stretching a specimen with oblate backbone anisotropy along the $\boldsymbol{e}_2$-axis, or if $s > 1$ and $1 < f < \sqrt{s}$, which coincides with stretching a specimen with prolate backbone anisotropy along the $\boldsymbol{e}_1$-axis. Motivated by the experiments performed by Kundler & Finkelman (1995), Talroze et al. (1998), and Zubarev et al. (1999), we assume hereafter that

$$s > 1 \qquad \text{and} \qquad 1 < f < \sqrt{s}. \tag{9.4}$$

9.2. *Inhomogeneous solutions*

The homogeneous solutions (9.2) correspond to fixed points of the differential equation (8.3). An eigenvalue analysis reveals that, of these, only the elliptic point $(9.2)_1$ may bifurcate into inhomogeneous solutions. Guided by the experiment of Kundler & Finkelmann (1995), where the undistorted state of the nematic elastomer corresponds to the trivial solution $\varphi = 0$, we focus attention on bifurcations that emanate from this point.

Linearizing (8.3) about $\varphi = 0$ and seeking solutions consistent with the boundary conditions (8.4), we find that bifurcations from $\varphi = 0$ may occur for critical values

$$f_n = \frac{\sqrt{l}}{(l^2 - \epsilon(s-1)n^2\pi^2)^{\frac{1}{4}}}, \tag{9.5}$$

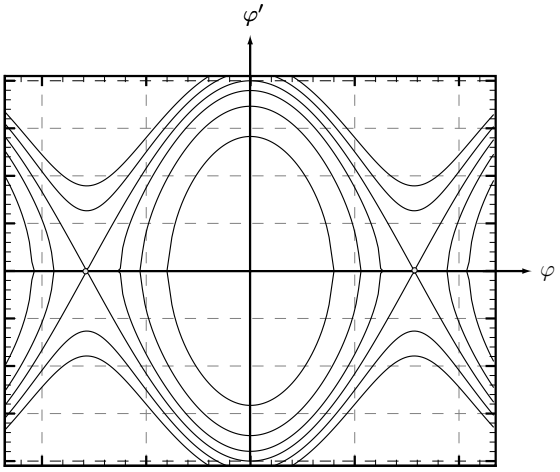

FIGURE 1. Schematic of the phase portrait for the equation (8.3). Due to the range $[-\frac{\pi}{2}, \frac{\pi}{2}]$ of φ, it is useful to think of the phase portrait as lying on the surface of a circular cylinder with axis along φ'. Elliptic points occur at $\varphi = 0$ and $\varphi = \frac{\pi}{2}$ (or, equivalently, $\varphi = -\frac{\pi}{2}$) and the hyperbolic points $\varphi = \pm \arcsin\left(\frac{1}{f}\sqrt{\frac{s(f^2-1)}{s-1}}\right)$ are connected by a heteroclinic orbit.

of the stretch f, where, by (9.4), the positive integer n obeys the inequality

$$n < \frac{l\sqrt{1+s}}{\sqrt{\epsilon}\pi s}. \tag{9.6}$$

Inhomogeneous solutions of (8.3)–(8.4) can then be constructed using the first integral

$$\varphi' \frac{\partial \tilde{\psi}(\gamma, \varphi, \varphi')}{\partial \varphi'} = \tilde{\psi}(\gamma, \varphi, \varphi') + \text{constant} \tag{9.7}$$

of (8.3). Specifically, as the first integral is constant along any solution of (8.3), all the solutions of the boundary-value problem correspond to level sets of (9.7) (see Figure 1). Due to the Neumann boundary conditions (8.4), these solutions must begin and terminate on the φ-axis of the phase portrait. Using the well-established argument involving the specimen's finite width l (see, for example, Cusumano, Sikora & Jester 1998), we conclude that only a finite number of such orbits serve as inhomogeneous solutions. Corresponding to an orbit that does exactly n half-turns about the central trivial solution there therefore exist periodic solutions

$$\varphi_n(x) = \pm a_n \cos\left(\frac{n\pi x}{l}\right) \tag{9.8}$$

describing a pair of states involving $n+1$ stripes separated by n transition layers. Across each such layer, the orientation and shear vary between the homogeneous values $(9.2)_{3_\pm}$ and $(9.3)_{3_\pm}$.

10. Local stability of inhomogeneous solutions

To obtain information concerning the local stability of the inhomogeneous solutions discussed above, we study the cubic approximation

$$\epsilon(s-1)\Big(1+\frac{1-s^2f^4}{s^2f^4}\varphi^2\Big)\varphi''+\epsilon(s-1)\Big(\frac{1-s^2f^4}{s^2f^4}\Big)|\varphi'|^2\varphi + \Big(1-\frac{1}{f^4}\Big)\varphi-\frac{2}{f^4}\Big(\frac{s-1}{s}+\frac{f^4-1}{3}\Big)\varphi^3=0 \quad (10.1)$$

of (8.3), which resembles the Euler equation of column buckling.

Introducing the local stretch parameter

$$\alpha_n = f - f_n, \quad (10.2)$$

we apply the Lyapunov–Schmidt method to (10.1) and obtain the bifurcation function

$$g(a_n,\alpha_n)=\frac{4f_na_n\alpha_n(l^2-\epsilon(s-1)n^2\pi^2)}{sl^2} - \frac{s^2(f_n^4-1)l^2+3s(s-1)l^2+\epsilon(s-1)(1-s^2f_n^4)n^2\pi^2}{2s^3f_n^2l^2}a_n^3+o(a_n^3), \quad (10.3)$$

with a_n the amplitude of the solution. On setting $g(a_n,\alpha_n)=0$, we arrive at

$$\alpha_n=\frac{s^2(f_n^4-1)l^2+3s(s-1)l^2+\epsilon(s-1)(1-s^2f_n^4)n^2\pi^2}{8s^2f_n^3(l^2-\epsilon(s-1)n^2\pi^2)}a_n^2+o(a_n^2). \quad (10.4)$$

A solution is locally stable or unstable depending on whether the derivative

$$\frac{\partial g(a_n,\alpha_n)}{\partial a_n}=\frac{4f_n\alpha_n(l^2-\epsilon(s-1)n^2\pi^2)}{sl^2} - \frac{3s^2(f_n^4-1)l^2+9s(s-1)l^2+3\epsilon(s-1)(1-s^2f_n^4)n^2\pi^2}{2s^3f_n^2l^2}a_n^2+o(a_n^2) \quad (10.5)$$

is negative or positive (Golubitsky 1988). For the trivial solution, which corresponds to the choice $a_n=0$, we have

$$\frac{\partial g(a_n,\alpha_n)}{\partial a_n}\Big|_{a_n=0}=\frac{4f_n\alpha_n(l^2-\epsilon(s-1)n^2\pi^2)}{sl^2}. \quad (10.6)$$

Hence, the trivial solution is stable or unstable depending on whether a_n is negative or positive, respecitively. Further, granted (10.4),

$$\frac{\partial g(a_n,\alpha_n)}{\partial a_n}=-\frac{s^2(f_n^4-1)l^2+3s(s-1)l^2+\epsilon(s-1)(1-s^2f_n^4)n^2\pi^2}{s^3f_n^2l^2}a_n^2, \quad (10.7)$$

and it follows that, once it comes into existence, the nontrivial solution corresponding to (10.4) is locally stable. This is a classicial exchange of stability: to the left of the bifurcation point, only the trivial solution is stable, whereas, to the right of the bifurcation point, stability is transferred to the non-trivial solution.

11. Thickness of the interstripe layer

Considering a state involving $n+1$ stripes, we assume that the n transition layers connecting these stripes have identical thickness. We describe a generic interstripe layer

as a set

$$\Big\{x : |\varphi'(x)| > \xi \max_{0<x<l} |\varphi'|\Big\}, \tag{11.1}$$

with ξ belonging to $(0,1)$ a dimensionless cut-off constant to be chosen, and write $\pm\varphi_n^*$ for the values of φ at the limits of the layer.

Following Fried & Grach (1998), we use first integral (9.7) to develop an analytical estimate for the thickness ℓ_n of an interstripe layer. We assume that the stretch f is close to a bifurcation point f_n, so that (9.8) yields a valid approximation for φ. Consistent with the scaling introduced in section 5, we assume also that $\sqrt{\epsilon}\,\varphi'$ is of the same order of magnitude as φ. Then, expanding (9.7) up to the third order in φ, we obtain

$$\epsilon(s-1)|\varphi'|^2 = \Big(1 - \frac{1}{f^4}\Big)(a_n^2 - \varphi^2). \tag{11.2}$$

which, upon separating variables, integrating over the layer and simplification, yields

$$\ell_n = \frac{2\sqrt{\epsilon(s-1)}f^2}{\sqrt{f^4-1}} \arcsin\Big(\frac{\varphi_n^*}{a_n}\Big). \tag{11.3}$$

From (11.2), it follows that

$$\max_{0<x<l} |\varphi'| = \sqrt{\frac{1}{\epsilon(s-1)}\Big(1 - \frac{1}{f^4}\Big)}\, a_n. \tag{11.4}$$

Invoking the definition (11.1) of the layer and using (11.4) in (11.2) then yields

$$\varphi_n^* = \sqrt{1-\xi^2}\, a_n. \tag{11.5}$$

Thus, by (11.3), the interstripe thickness is independent of the number of stripes and, writing

$$\ell = \ell_n, \tag{11.6}$$

we obtain the estimate

$$\ell = \frac{2\sqrt{\epsilon(s-1)}f^2 \arcsin\sqrt{1-\xi^2}}{\sqrt{f^4-1}}. \tag{11.7}$$

The lack of n-dependence in this estimate shows that the localization processes which gives rise to an interstripe layer is insensitive to the material state in the far field. On the other hand, the thickness of the layer shows tangible dependence upon the axial stretch f. This dependence stems from the factor of $\boldsymbol{F}^\top$ present in the gradient-energy density (3.6), a factor which gives rise to dependencies upon f and γ in the coefficient of $|\varphi'|^2$ in (6.5) and which is required (Anderson et al. 1999) to ensure invariance.

12. Energy of an interstripe layer

We now consider the problem of estimating the energy of a transition layer in a state involving $n+1$ stripes. We consider a generic interstripe layer centered at a point x_* and, accounting for the uniform elastic contribution arising from the first term on the right-hand side of (6.4), define the energy $\mathcal{E}_n$ of the layer by

$$\mathcal{E}_n = \int_{x_*-\frac{\ell}{2}}^{x_*+\frac{\ell}{2}} \Big(\frac{(f^2-1)^2}{2f^2} + \tilde{\psi}(\gamma,\varphi,\varphi')\Big)\, dx. \tag{12.1}$$

Taking for γ the expression (8.1), we expand $\tilde{\psi}$ up to the third order in φ and employ (11.2). This yields an approximation of $\tilde{\psi}$ in terms of φ. Inserting this expression in (12.1), we obtain

$$\mathcal{E}_n = \frac{(f^2-1)^2\ell}{2f^2} + \frac{(s-1)(f^4-1)a_n^2\ell}{2sf^2} + \frac{1}{2}\Big(\frac{f^4-(f^4-1)(2s+(s-1)a_n^2-1)}{sf^2} - \frac{sf^2}{s^2f^4+(s-1)(f^4-1)a_n^2}\Big)\int\limits_{x_*-\frac{\ell}{2}}^{x_*+\frac{\ell}{2}} \varphi^2\,dx. \quad (12.2)$$

To evaluate the integral on the right-hand side of (12.2), we use (11.2) to make a change of variables and find that

$$\int\limits_{x_*-\frac{\ell}{2}}^{x_*+\frac{\ell}{2}} \varphi^2 dx = \frac{\sqrt{\epsilon(s-1)}f^2\big(\arcsin\sqrt{1-\xi^2}-\xi\sqrt{1-\xi^2}\big)a_n^2}{\sqrt{f^4-1}}. \quad (12.3)$$

Thus, combining (12.2) with (12.3) and using (11.7), we determine an estimate

$$\mathcal{E}_n = \sqrt{\epsilon(s-1)}\Big(\frac{(f^2-1)\arcsin\sqrt{1-\xi^2}}{\sqrt{f^2+1}} + \mathcal{A}_n(f,s,\xi)\Big), \quad (12.4)$$

with

$$\mathcal{A}_n(f,s,\xi) = \Big(\frac{(s-1)\sqrt{f^4-1}\xi\sqrt{1-\xi^2}}{s} + \Big(\frac{1-(s-1)(f^4-1)a_n^2}{2s\sqrt{f^4-1}} - \frac{sf^2}{s^2f^4+(s-1)(f^4-1)a_n^2}\Big) \times \big(\arcsin\sqrt{1-\xi^2}-\xi\sqrt{1-\xi^2}\big)\Big)a_n^2, \quad (12.5)$$

for the energy of the layer. Unlike (11.7), (12.4) depends upon the number n of interstripe layers present through the amplitude a_n.

13. Numerical results

13.1. *Solution of the boundary-value problem (8.3)–(8.4)*

To illustrate the foregoing ideas, we take

$$\epsilon = 10^{-6}, \quad (13.1)$$

which corresponds to setting the characteristic length δ equal the stripe-width 10^{-5} m observed by Kundler & Finkelmann (1995) and chosing the shear modulus μ and the Frank modulus κ equal to 10^5 N/m^2 and 10^{-11} N, respectively. Further, we take

$$s = 2, \quad (13.2)$$

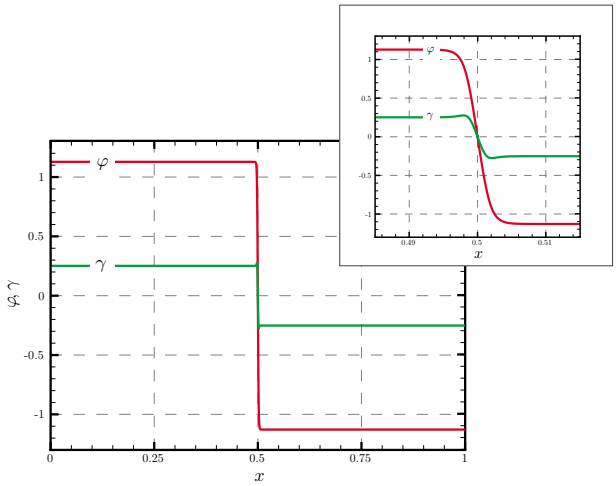

FIGURE 2. Plots of φ and γ for an inhomogeneous equilibrium solution with a single interstripe layer, computed for $\epsilon = 10^{-6}$, $l = 1$, $s = 2$, and $f = 1.3$. The layer is resolved in the subplot.

which corresponds to the step-length anisotropy present in the specimens of Kundler & Finkelmann (1995). By $(9.4)_2$, the choice (13.2) requires that the axial stretch f obey

$$1 < f < \sqrt{2}. \tag{13.3}$$

For simplicity, we assume that

$$l = 1 \tag{13.4}$$

and confine attention to solutions involving a single stripe, so that

$$n = 1. \tag{13.5}$$

Granted these choices, we solve the boundary-value problem (8.3)–(8.4) numerically for 414 equally spaced values of f ranging between 1 and 1.414. Figure 2 shows plots of the orientation and shear obtained for $f = 1.3$.

13.2. *Thickness of the interstripe layer*

With these numerically obtained solutions in place, we invoke the definition (11.1) with $\xi = \frac{9}{10}$ to compute the thickness ℓ_1 of the interstripe layer for each value of f. Figure 3 compares the numerically determined thicknesses with the the predictions of the estimate (11.7) specialized to the case $n = 1$. At the first bifurcation point, the layer is of considerable thickness. With increasing stretch, the layer thins and reaches a minimum near $f = 1.25$. The layer then thickens and reaches a limiting value at $f = 1.414$. Figure 3 shows that the asymptotic result (11.7) gives a remarkably good estimate of the layer thickness. However, the estimate decreases monotonically with f and, thus, fails to capture the local maximum exhibited by the numerical solution.

13.3. *Energy of the interstripe layer*

Using, once again, the numerically generated solutions and the definition (11.1) with $\xi = \frac{9}{10}$, we compute the energy $\mathcal{E}_1$ of the interstripe layer using the trapezoidal rule. Figure 4 compares the numerically determined energy with the predictions of estimate (12.4) specialized to the case $n = 1$. Both approaches indicate that $\mathcal{E}_1$ grows monotonically

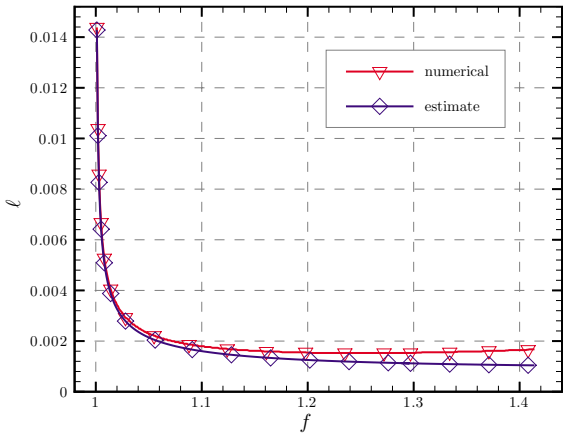

FIGURE 3. Thickness ℓ of the interstripe wall versus stretch f, computed in accordance with the definition (11.1), for $\epsilon = 10^{-6}$, $s = 2$, $n = 1$, and $\xi = \frac{9}{10}$ and compared to the predictions of the theoretical estimate (11.7) for $l = 1$, $n = 1$.

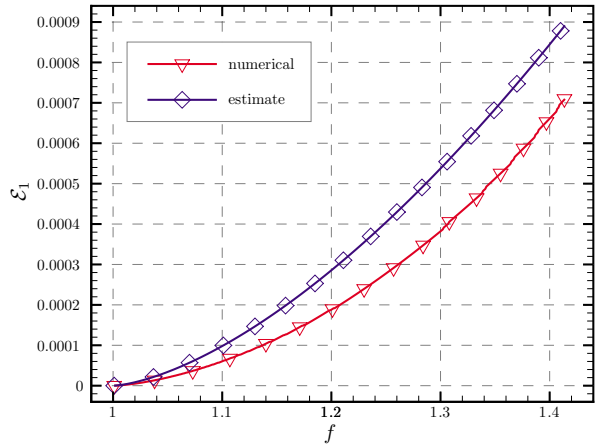

FIGURE 4. Free energy $\mathcal{E}_1$ of the interstripe layer versus stretch f, computed in accordance with the definition (11.1), for $\epsilon = 10^{-6}$, $s = 2$, and $\xi = \frac{9}{10}$ and compared to the predictions of the theoretical estimate (12.4) for $l = 1$, $n = 1$.

with f. As with the estimate for the thickness of the interstripe layer, the estimate (12.4) gives a remarkably good estimate of the energy of the interstripe layer. However, whereas (11.7) underestimates the thickness of the layer, (12.4) overestimates the energy of the layer.

14. Conclusions

Our results explain stripe formation in a clamped and unaixially extended nematic-elastomeric sheet as a bifurcation that occurs due to the need to accomodate extension while prohibiting macroscopic shear. We obtain analytical estimates of the thickness

and energy of interstripe layers and a comparison with numerical results obtained for a solution involving a single interstripe layer shows these estimates to be quite reliable over the entire interval of axial stretches. Nevertheless, the one-dimensional nature of our problem makes it impossible to predict the number of stripes present in a specimen of given thickness and, hence, the thickness of individual stripes.

Acknowledgments

We thank the National Science Foundation for support under Grant CMS 96-10286.

REFERENCES

Anderson, D. R., Carlson, D. E. & Fried, E., 1999. A continuum mechanical theory for nematic elastomers. *Journal of Elasticity* **56**, 33–58.

Cusumano, J. P., Sikora J. & Jester, W., 1998. Spatially periodic solutions in a 1D model of phase transitions with order parameter. *Physica D* **121**, 275–294.

Fried, E. & Grach, G., 1997. An order parameter-based theory as a regularization of a sharp interface theory for solid-solid phase transitions. *Archive for Rational Mechanics and Analysis* **138**, 355–404.

Golubitsky, M. & Schaeffer, D. G., 1985. *Singularities and groups in bifurcation theory*, v. 1. Springer-Verlag, New York.

Kundler, I. & Finkelmann, H., 1995. Strain-induced director reorientation in nematic liquid single crystal elastomers. *Macromolular Rapid Communications* **16**, 679–686.

Roberts, P. M. S., Mitchell, G. R. & Davis, F. J., 1997. A single director switching mode for monodomain liquid crystal elastomers. *Journal de Physique II* **7**, 1337–1351.

Talroze, R. V., Zubarev, E. R., Kuptsov, S. A., Merekalov, A. S., Yuranova, T., I., Plate, N. A. & Finkelmann, H., 1999. Liquid crystal acrylate-based networks: polymer backbone-LC order interaction. *Reactive & Functional Polymers*, **41**, 1–11.

Verwey, G. C., Warner, M. & Terentjev, E. M., 1996. Elastic instability and stripe domains in liquid crystalline elastomers. *Journal de Physique II* **6**, 1273–1290.

Warner, M., Gelling, K. P. & Vilgis, T. A., 1988. Theory of nematic networks. *Journal of Chemical Physics* **88**, 4008–13.

Zubarev, E. R., Kuptsov, S. A., Yuranova, T. I., Talroze, R. V. & Finkelmann, H., 1999. Monodomain liquid crystalline networks: reorientation mechanism from uniform to stripe domains. *Liquid Crystals*, **26**, 1531–1540.

List of Recent TAM Reports

No.	*Authors*	*Title*	*Date*
892	Fujisawa, N., and R. J. Adrian	Three-dimensional temperature measurement in turbulent thermal convection by extended range scanning liquid crystal thermometry—*Journal of Visualization* **1**, 355–364 (1999)	Oct. 1998
893	Shen, A. Q., E. Fried, and S. T. Thoroddsen	Is segregation-by-particle-type a generic mechanism underlying finger formation at fronts of flowing granular media?—*Particulate Science and Technology* **17**, 141–148 (1999)	Oct. 1998
894	Shen, A. Q.	Mathematical and analog modeling of lava dome growth	Oct. 1998
895	Buckmaster, J. D., and M. Short	Cellular instabilities, sub-limit structures, and edge-flames in premixed counterflows—*Combustion Theory and Modeling* **3**, 199–214 (1999)	Oct. 1998
896	Harris, J. G.	*Elastic waves*—Part of a book to be published by Cambridge University Press	Dec. 1998
897	Paris, A. J., and G. A. Costello	Cord composite cylindrical shells—*Journal of Applied Mechanics* **67**, 117–127 (2000)	Dec. 1998
898	Students in TAM 293–294	Thirty-fourth student symposium on engineering mechanics (May 1997), J. W. Phillips, coordinator: Selected senior projects by M. R. Bracki, A. K. Davis, J. A. (Myers) Hommema, and P. D. Pattillo	Dec. 1998
899	Taha, A., and P. Sofronis	A micromechanics approach to the study of hydrogen transport and embrittlement—*Engineering Fracture Mechanics* **68**, 803–837 (2001)	Jan. 1999
900	Ferney, B. D., and K. J. Hsia	The influence of multiple slip systems on the brittle–ductile transition in silicon—*Materials Science Engineering A* **272**, 422–430 (1999)	Feb. 1999
901	Fried, E., and A. Q. Shen	Supplemental relations at a phase interface across which the velocity and temperature jump—*Continuum Mechanics and Thermodynamics* **11**, 277–296 (1999)	Mar. 1999
902	Paris, A. J., and G. A. Costello	Cord composite cylindrical shells: Multiple layers of cords at various angles to the shell axis	Apr. 1999
903	Ferney, B. D., M. R. DeVary, K. J. Hsia, and A. Needleman	Oscillatory crack growth in glass—*Scripta Materialia* **41**, 275–281 (1999)	Apr. 1999
904	Fried, E., and S. Sellers	Microforces and the theory of solute transport—*Zeitschrift für angewandte Mathematik und Physik* **51**, 732–751 (2000)	Apr. 1999
905	Balachandar, S., J. D. Buckmaster, and M. Short	The generation of axial vorticity in solid-propellant rocket-motor flows—*Journal of Fluid Mechanics* (submitted)	May 1999
906	Aref, H., and D. L. Vainchtein	The equation of state of a foam—*Physics of Fluids* **12**, 23–28 (2000)	May 1999
907	Subramanian, S. J., and P. Sofronis	Modeling of the interaction between densification mechanisms in powder compaction—*International Journal of Solids and Structures*, in press (2000)	May 1999
908	Aref, H., and M. A. Stremler	Four-vortex motion with zero total circulation and impulse—*Physics of Fluids* **11,** 3704-3715	May 1999
909	Adrian, R. J., K. T. Christensen, and Z.-C. Liu	On the analysis and interpretation of turbulent velocity fields—*Experiments in Fluids* **29**, 275–290 (2000)	May 1999
910	Fried, E., and S. Sellers	Theory for atomic diffusion on fixed and deformable crystal lattices—*Journal of Elasticity* **59**, 67–81 (2000)	June 1999
911	Sofronis, P., and N. Aravas	Hydrogen induced shear localization of the plastic flow in metals and alloys—*European Journal of Mechanics/A Solids* (submitted)	June 1999
912	Anderson, D. R., D. E. Carlson, and E. Fried	A continuum-mechanical theory for nematic elastomers—*Journal of Elasticity* **56**, 33–58 (1999)	June 1999

List of Recent TAM Reports (cont'd)

No.	*Authors*	*Title*	*Date*
913	Riahi, D. N.	High Rayleigh number convection in a rotating melt during alloy solidification—*Recent Developments in Crystal Growth Research* **2**, 211–222 (2000)	July 1999
914	Riahi, D. N.	Buoyancy driven flow in a rotating low Prandtl number melt during alloy solidification—*Current Topics in Crystal Growth Research* **5**, 151–161 (2000)	July 1999
915	Adrian, R. J.	On the physical space equation for large-eddy simulation of inhomogeneous turbulence—*Physics of Fluids* (submitted)	July 1999
916	Riahi, D. N.	Wave and vortex generation and interaction in turbulent channel flow between wavy boundaries—*Journal of Mathematical Fluid Mechanics* (submitted)	July 1999
917	Boyland, P. L., M. A. Stremler, and H. Aref	Topological fluid mechanics of point vortex motions	July 1999
918	Riahi, D. N.	Effects of a vertical magnetic field on chimney convection in a mushy layer—*Journal of Crystal Growth* **216**, 501–511 (2000)	Aug. 1999
919	Riahi, D. N.	Boundary mode–vortex interaction in turbulent channel flow over a non-wavy rough wall—*Proceedings of the Royal Society of London A* (submitted)	Sept. 1999
920	Block, G. I., J. G. Harris, and T. Hayat	Measurement models for ultrasonic nondestructive evaluation—*IEEE Transactions on Ultrasonics, Ferroelectrics, and Frequency Control* **47**, 604–611 (2000)	Sept. 1999
921	Zhang, S., and K. J. Hsia	Modeling the fracture of a sandwich structure due to cavitation in a ductile adhesive layer—*Journal of Applied Mechanics* (submitted)	Sept. 1999
922	Nimmagadda, P. B. R., and P. Sofronis	Leading order asymptotics at sharp fiber corners in creeping-matrix composite materials	Oct. 1999
923	Yoo, S., and D. N. Riahi	Effects of a moving wavy boundary on channel flow instabilities—*Theoretical and Computational Fluid Dynamics* (submitted)	Nov. 1999
924	Adrian, R. J., C. D. Meinhart, and C. D. Tomkins	Vortex organization in the outer region of the turbulent boundary layer—*Journal of Fluid Mechanics* **422**, 1–53 (2000)	Nov. 1999
925	Riahi, D. N., and A. T. Hsui	Finite amplitude thermal convection with variable gravity—*International Journal of Mathematics and Mathematical Sciences* **25**, 153–165 (2001)	Dec. 1999
926	Kwok, W. Y., R. D. Moser, and J. Jiménez	A critical evaluation of the resolution properties of *B*-spline and compact finite difference methods—*Journal of Computational Physics* (submitted)	Feb. 2000
927	Ferry, J. P., and S. Balachandar	A fast Eulerian method for two-phase flow—*International Journal of Multiphase Flow*, in press (2000)	Feb. 2000
928	Thoroddsen, S. T., and K. Takehara	The coalescence–cascade of a drop—*Physics of Fluids* **12**, 1257–1265 (2000)	Feb. 2000
929	Liu, Z.-C., R. J. Adrian, and T. J. Hanratty	Large-scale modes of turbulent channel flow: Transport and structure—*Journal of Fluid Mechanics* (submitted)	Feb. 2000
930	Borodai, S. G., and R. D. Moser	The numerical decomposition of turbulent fluctuations in a compressible boundary layer—*Theoretical and Computational Fluid Dynamics* (submitted)	Mar. 2000
931	Balachandar, S., and F. M. Najjar	Optimal two-dimensional models for wake flows—*Physics of Fluids*, in press (2000)	Mar. 2000
932	Yoon, H. S., K. V. Sharp, D. F. Hill, R. J. Adrian, S. Balachandar, M. Y. Ha, and K. Kar	Integrated experimental and computational approach to simulation of flow in a stirred tank—*Chemical Engineering Sciences* (submitted)	Mar. 2000
933	Sakakibara, J., Hishida, K., and W. R. C. Phillips	On the vortical structure in a plane impinging jet—*Journal of Fluid Mechanics* **434**, 273–300 (2001)	Apr. 2000

List of Recent TAM Reports (cont'd)

No.	*Authors*	*Title*	*Date*
934	Phillips, W. R. C.	Eulerian space–time correlations in turbulent shear flows	Apr. 2000
935	Hsui, A. T., and D. N. Riahi	Onset of thermal–chemical convection with crystallization within a binary fluid and its geological implications—*Geochemistry, Geophysics, Geosystems*, in press (2001)	Apr. 2000
936	Cermelli, P., E. Fried, and S. Sellers	Configurational stress, yield, and flow in rate-independent plasticity—*Proceedings of the Royal Society of London A* **457**, 1447–1467 (2001)	Apr. 2000
937	Adrian, R. J., C. Meneveau, R. D. Moser, and J. J. Riley	Final report on 'Turbulence Measurements for Large-Eddy Simulation' workshop	Apr. 2000
938	Bagchi, P., and S. Balachandar	Linearly varying ambient flow past a sphere at finite Reynolds number—Part 1: Wake structure and forces in steady straining flow	Apr. 2000
939	Gioia, G., A. DeSimone, M. Ortiz, and A. M. Cuitiño	Folding energetics in thin-film diaphragms	Apr. 2000
940	Chaïeb, S., and G. H. McKinley	Mixing immiscible fluids: Drainage induced cusp formation	May 2000
941	Thoroddsen, S. T., and A. Q. Shen	Granular jets—*Physics of Fluids* **13**, 4–6 (2001)	May 2000
942	Riahi, D. N.	Non-axisymmetric chimney convection in a mushy layer under a high-gravity environment—In *Centrifugal Materials Processing* (L. L. Regel and W. R. Wilcox, eds.), in press (2000)	May 2000
943	Christensen, K. T., S. M. Soloff, and R. J. Adrian	PIV Sleuth: Integrated particle image velocimetry interrogation/validation software	May 2000
944	Wang, J., N. R. Sottos, and R. L. Weaver	Laser induced thin film spallation—*Experimental Mechanics* (submitted)	May 2000
945	Riahi, D. N.	Magnetohydrodynamic effects in high gravity convection during alloy solidification—In *Centrifugal Materials Processing* (L. L. Regel and W. R. Wilcox, eds.), in press (2000)	June 2000
946	Gioia, G., Y. Wang, and A. M. Cuitiño	The energetics of heterogeneous deformation in open-cell solid foams	June 2000
947	Kessler, M. R., and S. R. White	Self-activated healing of delamination damage in woven composites—*Composites A: Applied Science and Manufacturing* **32**, 683–699 (2001)	June 2000
948	Phillips, W. R. C.	On the pseudomomentum and generalized Stokes drift in a spectrum of rotational waves—*Journal of Fluid Mechanics* **430**, 209–229 (2001)	July 2000
949	Hsui, A. T., and D. N. Riahi	Does the Earth's nonuniform gravitational field affect its mantle convection?—*Physics of the Earth and Planetary Interiors* (submitted)	July 2000
950	Phillips, J. W.	Abstract Book, 20th International Congress of Theoretical and Applied Mechanics (27 August – 2 September, 2000, Chicago)	July 2000
951	Vainchtein, D. L., and H. Aref	Morphological transition in compressible foam—*Physics of Fluids* **13**, 2152–2160 (2001)	July 2000
952	Chaïeb, S., E. Sato-Matsuo, and T. Tanaka	Shrinking-induced instabilities in gels	July 2000
953	Riahi, D. N., and A. T. Hsui	A theoretical investigation of high Rayleigh number convection in a nonuniform gravitational field—*Acta Mechanica* (submitted)	Aug. 2000
954	Riahi, D. N.	Effects of centrifugal and Coriolis forces on a hydromagnetic chimney convection in a mushy layer—*Journal of Crystal Growth*, in press (2001)	Aug. 2000
955	Fried, E.	An elementary molecular-statistical basis for the Mooney and Rivlin–Saunders theories of rubber-elasticity—*Journal of the Mechanics and Physics of Solids*, in press (2001)	Sept. 2000

List of Recent TAM Reports (cont'd)

No.	*Authors*	*Title*	*Date*
956	Phillips, W. R. C.	On an instability to Langmuir circulations and the role of Prandtl and Richardson numbers—*Journal of Fluid Mechanics*, in press (2001)	Sept. 2000
957	Chaïeb, S., and J. Sutin	Growth of myelin figures made of water soluble surfactant—Proceedings of the 1st Annual International IEEE–EMBS Conference on Microtechnologies in Medicine and Biology (October 2000, Lyon, France), 345–348	Oct. 2000
958	Christensen, K. T., and R. J. Adrian	Statistical evidence of hairpin vortex packets in wall turbulence—*Journal of Fluid Mechanics* **431**, 433–443 (2001)	Oct. 2000
959	Kuznetsov, I. R., and D. S. Stewart	Modeling the thermal expansion boundary layer during the combustion of energetic materials—*Combustion and Flame*, in press (2001)	Oct. 2000
960	Zhang, S., K. J. Hsia, and A. J. Pearlstein	Potential flow model of cavitation-induced interfacial fracture in a confined ductile layer—*Journal of the Mechanics and Physics of Solids* (submitted)	Nov. 2000
961	Sharp, K. V., R. J. Adrian, J. G. Santiago, and J. I. Molho	Liquid flows in microchannels—Chapter 6 of *CRC Handbook of MEMS* (M. Gad-el-Hak, ed.) (2001)	Nov. 2000
962	Harris, J. G.	Rayleigh wave propagation in curved waveguides—*Wave Motion*, in press (2001)	Jan. 2001
963	Dong, F., A. T. Hsui, and D. N. Riahi	A stability analysis and some numerical computations for thermal convection with a variable buoyancy factor—*Geophysical and Astrophysical Fluid Dynamics* (submitted)	Jan. 2001
964	Phillips, W. R. C.	Langmuir circulations beneath growing or decaying surface waves—*Journal of Fluid Mechanics* (submitted)	Jan. 2001
965	Bdzil, J. B., D. S. Stewart, and T. L. Jackson	Program burn algorithms based on detonation shock dynamics—*Journal of Computational Physics* (submitted)	Jan. 2001
966	Bagchi, P., and S. Balachandar	Linearly varying ambient flow past a sphere at finite Reynolds number: Part 2—Equation of motion—*Journal of Fluid Mechanics* (submitted)	Feb. 2001
967	Cermelli, P., and E. Fried	The evolution equation for a disclination in a nematic fluid—*Proceedings of the Royal Society A*, in press (2001)	Apr. 2001
968	Riahi, D. N.	Effects of rotation on convection in a porous layer during alloy solidification—Chapter in *Transport Phenomena in Porous Media* (D. B. Ingham and I. Pop, eds.), Oxford: Elsevier Science (2001)	Apr. 2001
969	Damljanovic, V., and R. L. Weaver	Elastic waves in cylindrical waveguides of arbitrary cross section—*Journal of Sound and Vibration* (submitted)	May 2001
970	Gioia, G., and A. M. Cuitiño	Two-phase densification of cohesive granular aggregates	May 2001
971	Subramanian, S. J., and P. Sofronis	Calculation of a constitutive potential for isostatic powder compaction—*International Journal of Mechanical Sciences* (submitted)	June 2001
972	Sofronis, P., and I. M. Robertson	Atomistic scale experimental observations and micromechanical/continuum models for the effect of hydrogen on the mechanical behavior of metals—*Philosophical Magazine* (submitted)	June 2001
973	Pushkin, D. O., and H. Aref	Self-similarity theory of stationary coagulation—*Physics of Fluids* (submitted)	July 2001
974	Lian, L., and N. R. Sottos	Stress effects in ferroelectric thin films—*Journal of the Mechanics and Physics of Solids* (submitted)	Aug. 2001
975	Fried, E., and R. E. Todres	Prediction of disclinations in nematic elastomers—*Proceedings of the National Academy of Sciences* (submitted)	Aug. 2001
976	Fried, E., and V. A. Korchagin	Striping of nematic elastomers—*International Journal of Solids and Structures* (submitted)	Aug. 2001